

ACTIVE AXIAL ELECTROMAGNETIC DAMPER

Alexei V. Filatov, Larry A. Hawkins
Calnetix Inc., Cerritos, CA, 90703, USA
afilatov@calnetix.com

Venky Krishnan, Bryan Lam
Direct Drive Systems Inc., Cerritos, CA, 90703, USA
ykrishnan@directdrivesystems.net

ABSTRACT

In magnetic bearing applications with rather limited axial loads and/or relaxed requirements for the axial positioning accuracy of the rotor it can be attractive to achieve the axial suspension using passive reluctance centering. In this case, however, it might be difficult to obtain the damping necessary to limit transient response to unexpected dynamic loads. A concept of an active electromagnetic axial damper developed for a 1MW 15,000RPM motor on magnetic bearings with passive axial reluctance centering is presented. The damper features a PM-biased actuator with a flux feedback. Using the flux feedback allows reducing the negative axial stiffness of the actuator to a level sufficient for using it in combination with a passive axial bearing exhibiting rather low positive axial stiffness 2400 lbf/in (420kN/m). The other advantages of the flux feedback include more linear relationship between the output force and the control command than in conventional current control as well as significant reduction of the gain and phase roll offs caused by the eddy currents. The design delivers 8760 N·s/m damping coefficient, which represents 20% of the critical damping, and 670N load capacity sufficient to address the worst-case-scenario dynamic response.

INTRODUCTION

Many direct-drive high-speed compressors, expanders and other machines utilize an arrangement where a turbine or a similar component is coupled through a flexible coupling to a high-speed motor or generator. One advantage of such an arrangement is that a single

motor/generator design can be utilized in several different machines. Another advantage is that both motor/generator and the turbine can be designed to operate below the first lateral rotor bending mode. The main disadvantage is that both the motor/generator and the turbine need separate sets of bearings. If magnetic bearings are used to support the rotor of the motor/generator, an attractive solution is to use passive reluctance centering for the axial rotor positioning, since it is a simpler (no external controls are needed), more compact and less expensive solution than a dedicated AMB. Additionally, using a compliant suspension on one of the coupled machines can facilitate alignment and reduce sensitivity to thermal growth.



Figure 1. 1MW 15kRPM PM Motor on Magnetic Bearings.

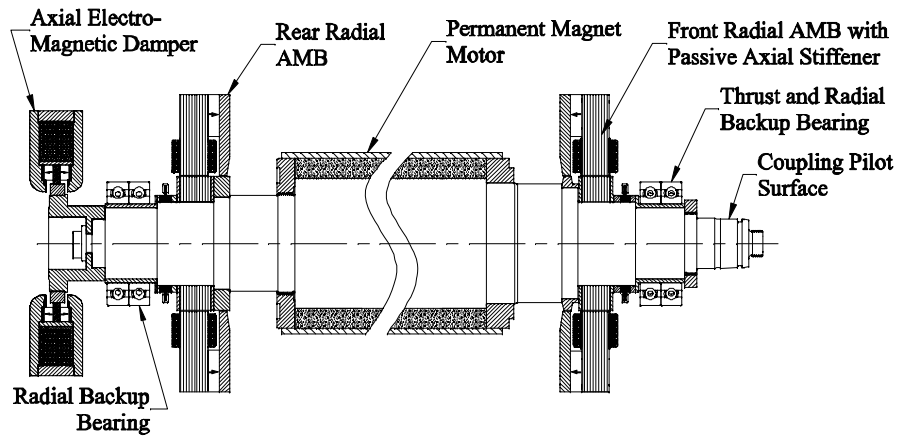


Figure 2. Layout of a 1MW 15kRPM motor on magnetic bearings.

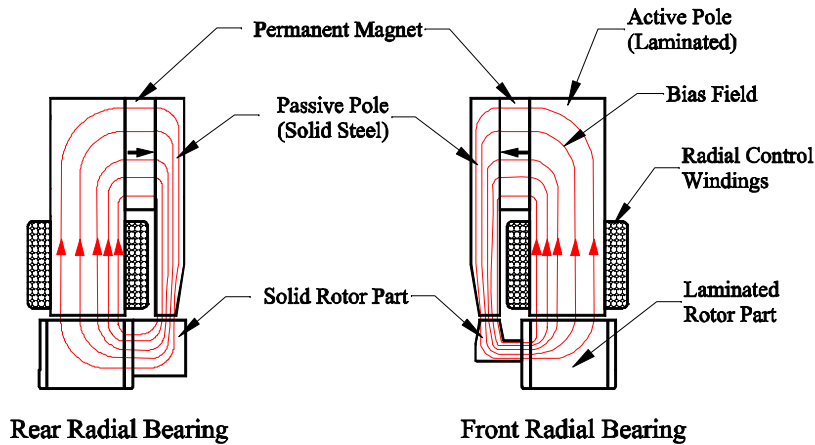


Figure 3. Bias flux distribution in the front and rear radial bearings.

This approach has been implemented in a new 1MW 15kRPM permanent-magnet motor developed by Direct Drive Systems and Calnetix for use in coupled applications (Figure 1). A schematic layout of this machine is shown in Figure 2. It utilizes two patented radial homopolar PM-biased Active Magnetic Bearings (AMBs) similar to the ones described in [1]. The main difference between the magnetic bearing system presented in [1] and the system shown in Figure 2 is that the passive stator pole of the front radial magnetic bearing shown in Figures 2 and 3 is tapered towards the shaft where it faces a similarly shaped solid rotating pole. The profiles of the stationary and rotating poles are chosen so that any axial rotor deflection from the position where these two poles are aligned causes

increase of the air gap reluctance resulting in a restoring axial force (positive axial stiffness). Furthermore, the value of this axial stiffness is maximized because the bias flux is compressed at the tips of the poles. According to Earnshaw's theorem, increase of the positive axial stiffness results in an increase of the negative radial stiffness, however, the impact is small and has not introduced noticeable problems.

In contrast to the front bearing, the rotating pole of the rear bearing is not tapered. Because of this, there is no reluctance change when the rotating pole moves axially with respect to the stationary pole, and, therefore, the rear magnetic bearing has no axial stiffness. Thus when the rotor heats up during operation, it is located axially by the front bearing and grows freely through the rear

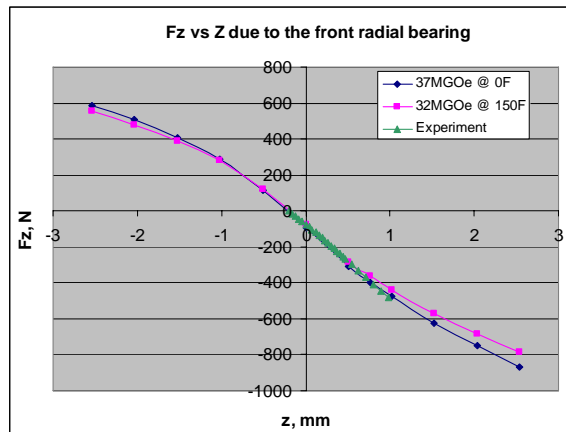


Figure 4. FEA-calculated axial force exerted on the rotor by the front AMB as a function of the axial position of the rotor (z) for two different combinations of the magnet strength and temperature.

bearing. The only reason that a tapered stationary pole has been used in the rear bearing as well was to reduce number of different parts in the system.

Figure 4 shows FEA-calculated axial reaction force versus position curves for the front AMB for two different combinations of the magnet strength and temperature as well as experimental data. Since the total bias flux is limited by saturating both stationary and rotating solid poles in the tapered areas, the magnet properties have little effect on the axial force. The positive axial stiffness estimate, based on the data shown in Figure 4 for the nominal rotor position ($z=0$), is approximately 2400 lbf/in (420kN/m). With the rotor weighing 396 lbf (180kg), the natural frequency of the axial oscillations in a standalone machine was expected to be around 7.7 Hz. Figure 5 shows an axial transient process observed following a hammer impact. The measured oscillation frequency was around 8.7Hz. This measurement indicates a net axial stiffness of 3,100 lb/in (545 kN/m). The difference should be due to a combination of unmodelled passive axial stiffness in the motor and any under prediction of the reluctance centering of the magnetic bearing. The measurement results also indicated that the damping is small as expected – approximately 2.2% of the critical damping. This damping is adequate for normal operation but insufficient to limit axial motion in the event of a high amplitude upset near the rigid body natural frequency. In most coupled application the coupling axial stiffness may significantly exceed the passive axial stiffness

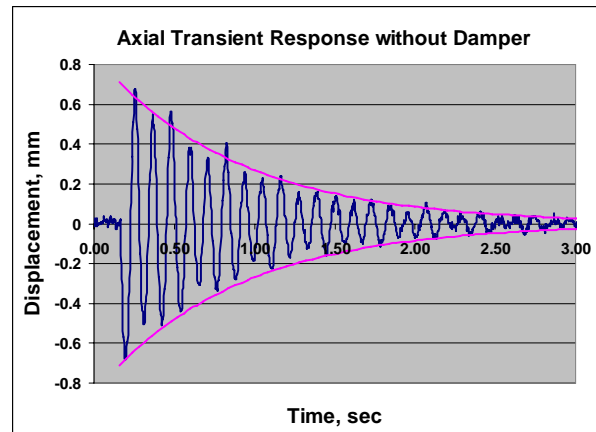


Figure 5. Axial rotor oscillations in a standalone motor following a hammer impact.

introduced by the front magnetic bearing. For example, in the primary targeted application, the motor will be driving a compressor supported by its own 5-DOF AMB system with the coupling between the motor and the compressor having axial stiffness of 12,000 lbf/in (2MN/m). Because of the mechanical coupling contribution to the suspension stiffness, the inherent axial damping of the motor rigid body mode is expected to be even a smaller percentage of the critical damping – roughly 1%. Since a compressor has the possibility of going into surge at low frequencies, the response of the motor to large amplitude motion of the compressor rotor was examined. Figure 6 shows the predicted axial frequency response of the motor rotor to the oscillations of the compressor rotor with 0.010 in (0.25mm) amplitude. The transmissibility from the compressor to the motor is fairly low except around the 17 Hz axial resonance where response amplitude may exceed 0.39in (10mm), with the acceptable limits being 0.0235in (0.6mm). Therefore, to prevent motor backup bearing impact in this worst-case scenario, considerably more axial damping would be needed. In order to limit the amplitude of the motor rotor oscillations to the desired level, at least 20% of the critical damping or 50 lbf-s/in (8760 N-s/m) was found to be needed. The maximum force that might be required from a damper was estimated as 115 lbf (520N).

DESIGN OF AN AXIAL ELECTROMAGNETIC DAMPER

As shown in the Figure 2, the most convenient place in the machine to accommodate the axial damper was on the rear end of the machine (opposite to the coupling).

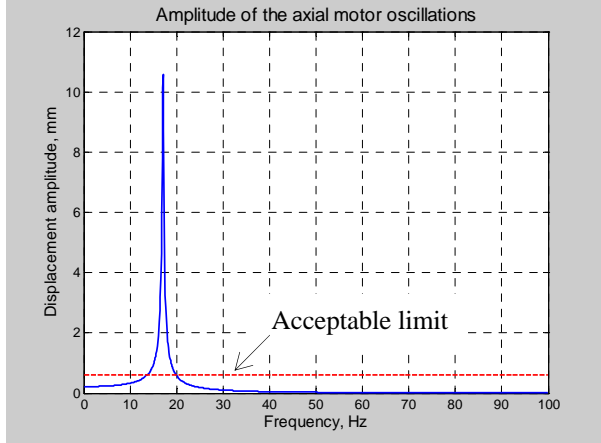


Figure 6. Axial frequency response of the motor rotor to the axial oscillations of a compressor rotor with 0.25mm amplitude and the axial damping equal to 1% of the critical damping.

This placement also allows the damper to be optionally installed – the machine can be run without a damper and later it can be installed without a teardown of the machine. One of the difficulties with the damper design was that because of the rotor thermal expansion during operation, the rear end of the rotor can be displaced with respect to the stator by almost 0.08in (2mm). Considering that the positive axial stiffness produced by the front magnetic bearing was rather limited, the damper could not be allowed to have a significant negative axial stiffness. As a solution, it was proposed to use a novel PM-biased electromagnetic actuator with flux feedback. Its principle of operation is illustrated in Figure 7.

The axial force exerted on the actuator target shown in Figure 7 can be presented in the first approximation as

$$F_z = \frac{A}{2\mu_0} (B_2^2 - B_1^2) A \quad \text{or}$$

$$F_z = \frac{A}{2\mu_0} (B_2 - B_1) \cdot (B_2 + B_1)$$

where B_2 and B_1 are flux densities in the axial air gaps #2 and #1 respectively and A is an effective area of the target face.

As it can be seen from Figure 7, in the air gap #2 the bias and the control fluxes are added, while in the gap #1 they are subtracted from each other, i.e.

$$B_2 = B_b + B_c; \quad B_1 = B_b - B_c$$

Therefore, equation (1) can be rewritten as

$$F_z = \frac{A}{\mu_0} B_b \cdot (B_2 - B_1)$$

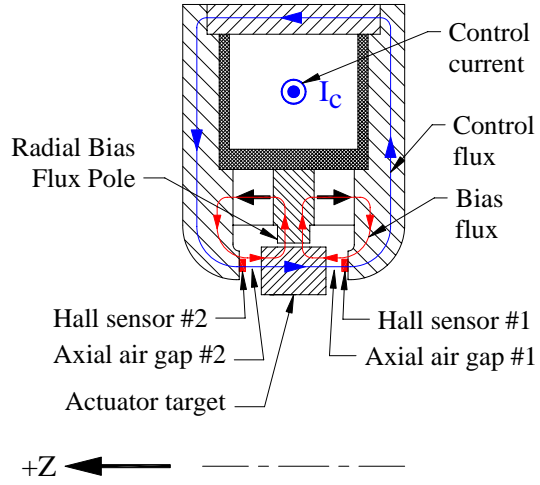


Figure 7. Structure and operational principle of the proposed electromagnetic actuator with a flux feedback.

The bias flux density defined as $B_b = 0.5 \cdot (B_1 + B_2)$ in this actuator is essentially independent of the operating conditions, including temperature, target position, control current, etc. because the net bias flux is defined by the cross-sectional area of deeply saturated Radial Bias Flux Pole. This does not mean that either B_1 or B_2 will stay constant when for example the target is moved axially or when a control current is applied; however their sum will. Therefore, the axial force F will be directly proportional to the difference in the flux densities $B_2 - B_1$ measured with Hall sensors installed in the air gaps. The fact that the output force is simply proportional to the measured signal is one of the significant advantages of the proposed scheme compared to other known implementations of the flux feedback [2]. The other important advantage is that the control flux does not have to travel through high-reluctance permanent magnets. This results in a more compact and energy efficient device.

A local actuator control loop (Figure 8) sets the current I_z in the control coil to make the difference $B_2 - B_1$ proportional to the actuator input command U_{com} . If U_{com} is proportional to the negative of the axial velocity of the rotor, i.e. $U_{com} \sim -V_z$, then F_z will be nearly proportional (subject to the control accuracy) to $-V_z$, as desired from a damper.

The advantages of the flux feedback control over a more conventional current control include:

- 1.) Practical elimination of the actuator negative stiffness;

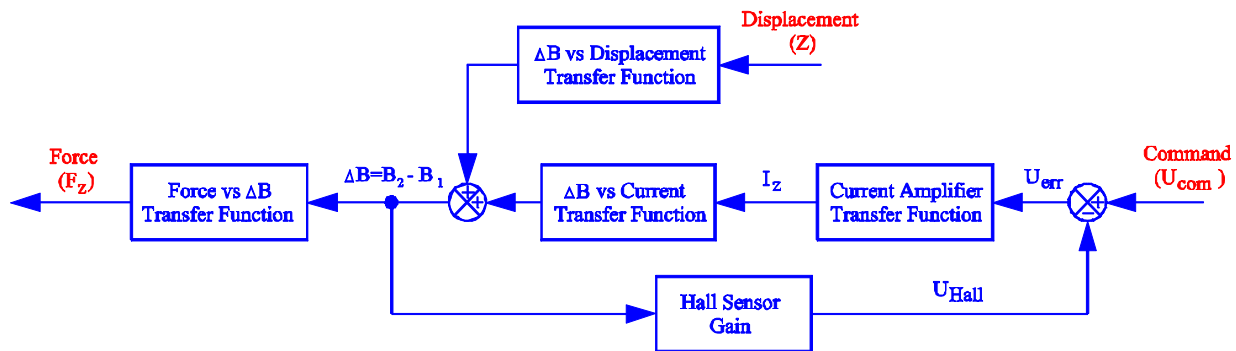


Figure 8. Control loop of the actuator with field feedback.

- 2.) The force remains a linear function of $B_2 - B_1$ all the way up to the material saturation point;
- 3.) Much more uniform actuator transfer function over a wide frequency range.

For the current application in a damper, probably the most important advantage is elimination of the negative stiffness. In the control loop shown in Figure 8 the negative stiffness is accounted for by using the “ ΔB vs Displacement” block. For example, if the actuator target is shifted in the positive Z direction, then B_2 becomes larger than B_1 producing a force also acting in the positive z direction. Note, however, that the force still will be proportional to $\Delta B = B_2 - B_1$ and if ΔB is controlled to zero then the force will be nearly zero regardless of the rotor position.

Figure 9 shows negative stiffness force before and after activating the flux feedback mode calculated with FEA. It can be seen that in the flux feedback mode the negative stiffness forces are reduced by approximately an order of magnitude.

Figure 10 illustrates another advantage of the flux feedback mode: more linear dependence of the output force vs command signal (control current in the current control mode or ΔB in the flux-feedback mode).

Yet another advantage of the flux-feedback mode is a more uniform transfer function over a wide frequency range. Since axial actuators typically rely on a non-laminated iron, their force/current transfer functions are strongly affected by the eddy currents induced in the iron. For example, Figure 11 shows the flux distribution in the proposed actuator at 0Hz and at 10Hz. At 10Hz a significant portion of the magnetic flux is expelled from the iron due to the skin effect. As a result, less flux is generated in the axial gaps at 10Hz than at 0Hz even though the same control current amplitude is used. It

can be noticed, however, that even though the magnetic flux distribution becomes very non-uniform inside the iron at high frequencies, it remains rather uniform inside the air gaps. Therefore, knowing $\Delta B = B_2 - B_1$ still will allow rather accurate prediction of the axial force exerted on the actuator target. In addition to the gain roll off, eddy currents also cause a phase lag between the control current and the control flux (and, consequently, the output force), which further complicates the system control. Using the flux feedback allows to reduce negative effects of both the gain and phase roll off in the actuator transfer functions caused by the eddy currents. Figure 12 compares the damper actuator transfer functions calculated for the

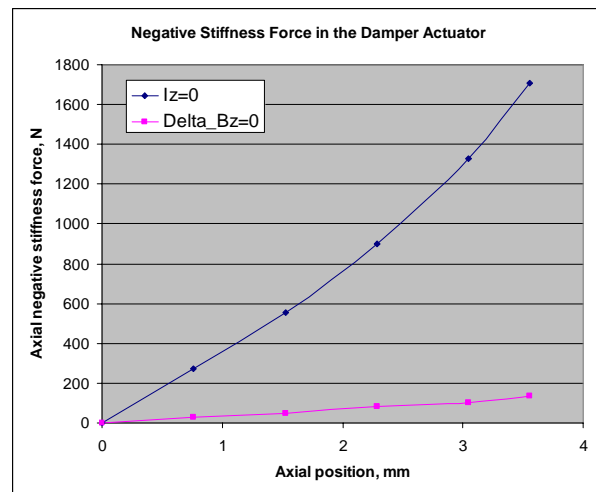
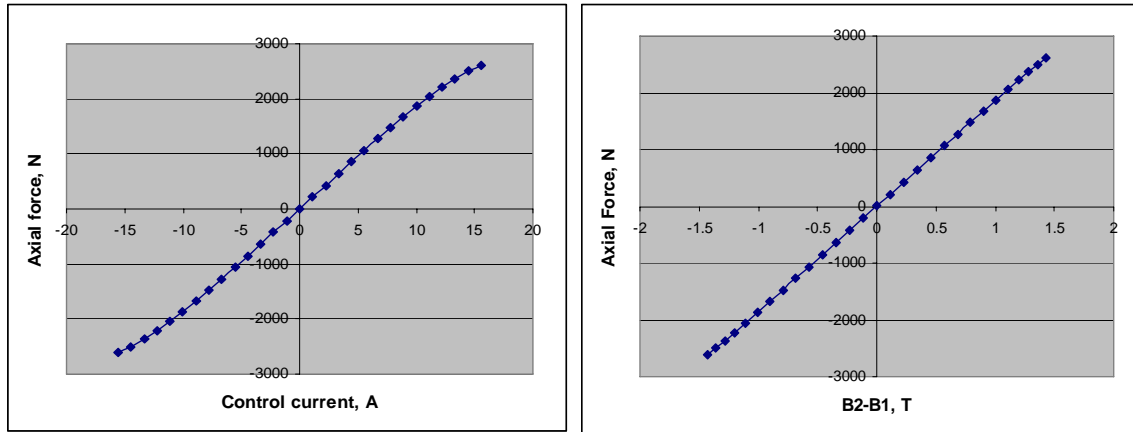


Figure 9. Comparison of the negative stiffness forces developing in the axial actuator before activating the flux feedback mode ($I_z=0$) and after ($\Delta B_z=0$).



Current control

Flux-Feedback control

Figure 10. Comparison of the output force vs command input relationships when the actuator is operated in the current control (left) and the flux-feedback (right) mode. The command input in the current control mode is the control current, in the flux feedback mode – flux density difference ($B_2 - B_1$).

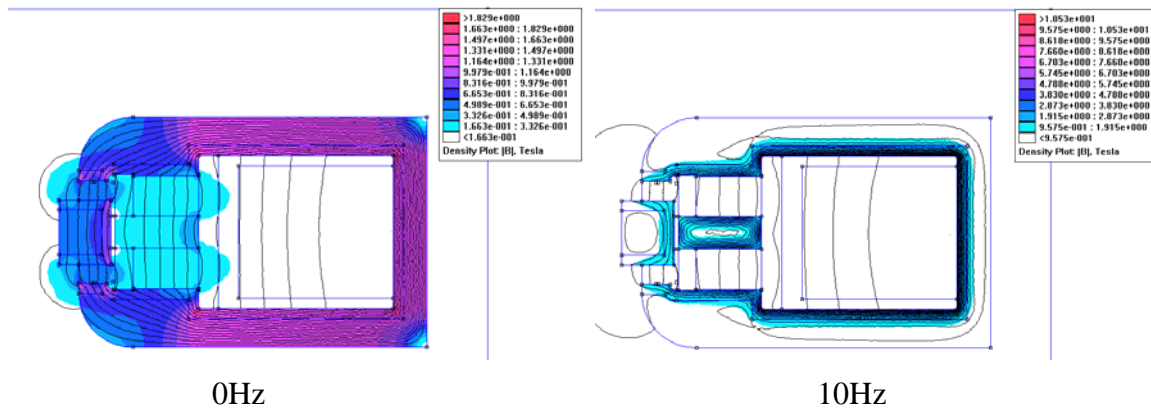


Figure 11. Control flux distribution in the actuator at 0Hz and at 10Hz.

conventional current control and the flux feedback controls. It can be noticed that in the flux feedback mode both gain and phase stay nearly constant up to 100Hz, whereas in the conventional current-control mode there would be significant losses of both the gain and the phase.

Regarding practical implementation of the proposed actuator, its main drawback is that installing Hall-effect sensors in the axial air gaps in most cases would require the gaps to be considerably larger than normal; however in the current applications the axial air gaps had to be very large anyway (nominal gap close to 0.2in (5mm) on each side) in order to accommodate the large expected thermal expansion and dynamic motion

of the rotor. Compared to the nominal gap, the 0.6-mm thickness of Hall sensors used in the damper design is rather small. Having very large air gaps was further facilitated by using permanent magnets to generate the bias field, since they offer significant space saving compared to current-carrying coils.

Currently the damper is under final stages of the construction and will be tested soon.

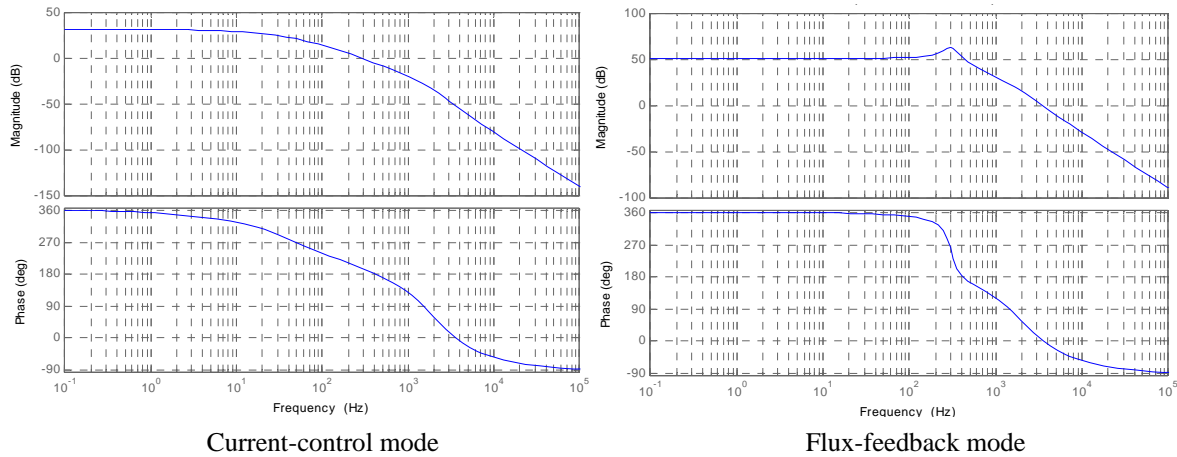


Figure 12. Actuator transfer functions in the current-control mode and the flux-feedback mode.

CONCLUSIONS

The proposed axial PM-biased actuator with a flux-feedback control is shown to have several important advantages over more conventional current-controlled actuators including

- 1.) Practical elimination of the actuator negative stiffness;
- 2.) The force remaining a linear function of the command signal all the way up to the material saturation point;
- 3.) Uniform actuator transfer function over a wide frequency range.

In particular, this design allows an easy implementation of an axial damper in magnetic bearing systems utilizing passive axial reluctance centering. Such systems are very attractive for coupled applications mainly because making the suspension of one of the coupled machines more compliant significantly facilitates the alignment and operation, but also because they offer a more compact, simple, reliable and less expensive solution than a dedicated axial AMB channel.

ACKNOWLEDGEMENT

All the finite element simulations presented in this paper have been carried out with FEMM – a program for electromagnetic analysis developed by Dr. D. Meeker (<http://femm.foster-miller.com>).

References

1. Filatov, A., McMullen, P, Hawkins L. and Blumber E., Magnetic Bearing Actuator Design for a Gas Expander Generator, Proc. of the 9th Int. Symp. On Magnetic Bearings, Lexington, KY, USA, Aug. 2004.
2. Groom, N., Permanent Magnet Flux-Biased Magnetic Actuator with Flux Feedback, US Patent No. 5,003,211, Mar. 26, 1991